

A NOVEL ROBUST TECHNIQUE FOR THE MEASUREMENT OF LIQUID PHASE VELOCITY IN TWO-PHASE BUBBLY FLOWS USING PARTICLE IMAGE VELOCIMETRY

Rafael F. L.de Cerqueira

Emilio E. Paladino

Bruno K. Ynumaru

SINMEC - Computational Fluid Dynamics Lab

Mechanical Engineering Department

Federal University of Santa Catarina

88040-900 - Florianopolis - SC - Brazil

rafaelfc@sinmec.ufsc.br, paladino@sinmec.ufsc.br, ynumaru@gmail.com

Abstract. Particle Imaging Velocimetry (PIV) measurement in gas-liquid bubbly flows is a challenging task, mainly due to the dispersion of the laser light caused by the gas-liquid interfaces. A common solution adopted is the use of fluorescent seeding particles associated with a bandpass filter for the laser light. Therefore, the camera captures only the light fluoresced by the seeding particles, filtering the laser light dispersed by the gas-liquid interfaces and measuring a velocity field which corresponds to the liquid phase, where particle seeding occurs. However, even for relatively low gas fractions, the fluoresced light reflected by the interfaces distorts the measurements, due to the fact that the reflected particles are out from the laser plane. In addition, the fluoresced light also reflects at the interfaces, distorting the measurements and trending to overshoot the measured liquid velocities. In this work, PIV measurements of air water bubbly flows are performed with fluorescent tracer particles (PIV/LIF). A method was developed to overcome the problems caused by the presence of bubbles in the flow, which uses the pixel intensity information of the interrogation window from each velocity vector. The proposed method was tested for three air-water flow configurations, from low to moderate void fractions (up to approximately 9.0 %). From the two-phase flow experiments, the method described in this work is capable to measure the liquid velocity and it is shown that without the correct treatment, the void fraction can be overestimated.

Keywords: Particle Image Velocimetry, Multiphase flow, Bubbly flow

1. INTRODUCTION

In gas-liquid bubbly flow, the liquid velocity and its fluctuating components are fundamental for the comprehension of the flow behavior and to study the effect of the gas-phase in the turbulence parameters. Therefore, it is important to gather experimental data which can give insight to local flow patterns, such as wakes and recirculation regions induced by the gas-liquid interactions, and also to provide averaged values that can be used in closure relations. Another use of these experimental studies is to provide reliable data that can aid CFD two-phase modeling and validate its results.

Experimental data for bubbly flows using Laser Doppler Velocimetry (LDV) (Hosokawa and Tomiyama, 2013; Sun *et al.*, 2004a,b) can be found in the literature. However, as the void fraction increases, the techniques cannot be applied due to the large concentration of bubbles and the variation of its size and shape. In the last two decades, the Particle Image Velocimetry (PIV) has been used as a measurement technique for two-phase flows.

In order to use the PIV method in two-phase flows, specially in bubbly flows, additional effort is needed due to the presence of the liquid-gas interfaces, turning this kind of measurements significantly more complicated when compared to single-phase flows. Most of the experimental studies are focused in the liquid velocity, and since the images acquired by the camera consists of the two phases, some additional steps are needed to distinguish the liquid and the dispersed gas phase.

In the work of Bröder and Sommerfeld (2002), the authors develop a method based in an experimental setup of two synchronized cameras, each with different optical filters. One optical arrangement is used to capture only the tracer in the liquid phase and the other to acquire only the dispersed bubbly phase. This setup was used in a bubble column with a gas hold-up which varied in the range between 0.5 and 19.0%. However, the method can only be used when the diameter of the bubbles is small when compared to dispersed bubbles, such as the case of a bubble column.

An experimental procedure for phase separation is presented by Lindken and Merzkirch (2002), which consists in the use of PIV in combination with laser-induced fluorescence (LIF) and pulsed shadowgraphy. In this work, the LIF technique helps to visualize the liquid tracer particles by the use of fluorescent particles and narrow band optical filters. The phase discrimination is done by the pulsed shadowgraphy technique, which can be used to calculate the bubble shape

and size, creating a "binary mask" from the gas phase that can be subtracted of the original captured image. The same experimental procedure is used by Fujiwara *et al.* (2004) to study the vertical upward driven bubbly pipe flow with void fractions of 0.5 % to 1.0 % and by (Kim *et al.*, 2016) to characterize the bubble-induced turbulence in a laminar upward flows with void fractions ranging of 0.05 % to 0.64 %. This technique is restricted to bubbly flows with low gas fractions, due to the fact that the phase discrimination is done volumetrically, while the PIV method uses a planar light sheet to capture the seed particles.

The work of Bröder and Sommerfeld (2007) circumvents the low gas fraction limitation by using macro optics in the CCD camera, thereby achieving a small depth of field and making possible, by a method based in the gradient of gray values, to discriminate between bubbles inside and outside the camera's focal plane. Using these additional procedures the authors can study gas-liquid bubbly flows inside a bubble column with a range between 0.5 and 5.0% of gas volume fraction.

The method described in Zhou *et al.* (2013), on the contrary of the described method of the paragraphs above, does not make use of additional cameras or pulsed the shadowgraphy technique, it only requires the PIV-LIF for the optical phase separation. The phase discrimination is done through the image processing of the raw PIV-LIF images and can be used for liquid-gas pipe flow with a void fraction up to 18.0%. A great advantage of the proposed method is the fact that all calculations are done in a "planar" fashion, since it uses the raw PIV images acquired with the light sheet illumination. However, the method creates PIV a synthetic binary image, in which the discrimination of the tracer particles and the dispersed bubbles is done through a geometric and shape criteria from a processed binary image. This parameter is chosen manually and can introduce errors in the cross-correlation PIV procedure used for the liquid velocity calculation.

Considering the methods described in the literature and their limitations, a new method for the measurement of the liquid phase velocity in two-phase pipe bubbly flows using the PIV-LIF technique is described, which is capable to extract reliable experimental data with void fractions up to 9.0%. After the introduction of the experimental setup, the measuring technique and the problems arising from the two-phase flows measurement are discussed, then the proposed method is presented. Finally, results concerning the time-averaged two-phase bubbly flows are discussed upon their reliability and accuracy.

2. EXPERIMENTAL SETUP

This section describes the experimental setup used in this work. This system allows for the generation of a single-phase liquid stream or bubbly flow in a straight vertical duct, where the water and air flow rates can be controlled. Thus, the superficial velocities of liquid and dispersed bubbles phase can be independently controlled.

The experimental apparatus is schematically depicted in Figure 1. The test section consists of a 26.2 mm internal diameter by 2.0 m length of a transparent duct. A two-phase stream is generated at the bottom of the test section by combining a liquid stream (tap water), driven by a centrifugal pump, and air from the compressed air line from the building. To eliminate oil and solid particles, air is treated and pressure is maintained constant at the injection point through a pressure regulating valve, making it independent of the line demand. The dispersed bubbles are injected in the bottom of the tube, and the gas superficial velocity is measured by two OMEGA FL-3802ST/FL-3861SA flow meters with ranges of 81.4-814.0 standard mL/min and 26.3-263.0 standard mL/min, both with $\pm 2.0\%$ full scale accuracy. The flow rate is controlled by a needle valve downstream. In order to correct the gas superficial velocity due to gas expansion, a pressure and a temperature sensor were installed downstream the needle valves. As the return to the reservoir consists of a relatively short, 50.0 mm internal diameter duct, and the reservoir is opened to the atmosphere, it was assumed that the pressure at the test section was close to the atmospheric pressure. Thus, the pressure difference between the test section and the flow meter was considered equal to the manometric pressure at the flow meter section. A porous gas diffuser was installed in the bottom of the tube, in order to control the sizes of the dispersed bubbles. The water flow rate is measured by an OMEGA FL46303 flow meter with range of 1.00-7.50 l/min with $\pm 5.0\%$ full scale accuracy. The liquid flow rate is controlled through a frequency inverter connected to the electric water pump motor.

At the PIV measurement section, a box constructed with transparent acrylic, made with 8 faces, filled with the water is included to avoid optical distortion.

3. MEASUREMENT TECHNIQUE

The PIV technique is largely described in literature (e.g., Raffel *et al.* (2007)) and will not be described here. The PIV system available at SINMEC Lab consist of a 2048x2048 pixels (4 MPx) resolution CCD camera, a pulsed Nd:YAG laser with a wavelength of 532 nm and a synchronizer to match the emission of laser pulses and image capturing, which can be externally triggered. For all the experiments done in this work, the time difference between the two consecutive frames for vector analysis, Δt , was defined as 1000.0 μs . For the PIV image data, the interrogation size was maintained constant at 32 x 32 pixels throughout the experiments and these were overlapped by 50 %. From the acquired consecutive frames, the Fast Fourier Transform (FFT) cross-correlation of the TSI Insight 4G software was used to generate the vector fields and to remove spurious velocity vectors. The signal-to-noise ratio (SNR) was set to 2.0, in order to remove those spurious

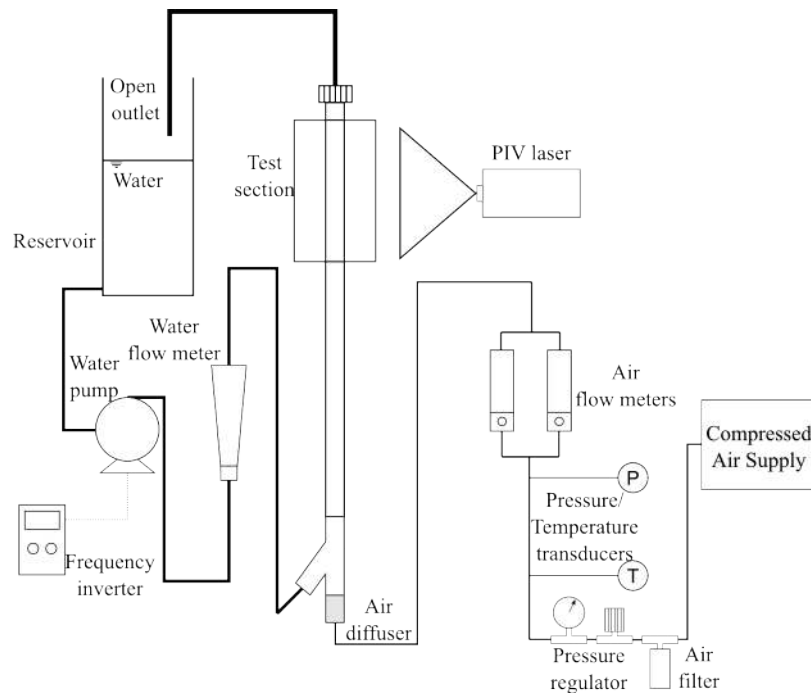


Figure 1: Experimental setup.

vectors.

In applications to gas-liquid flows, the presence of the interfaces with much larger scales than the seeding particles, scatters the light of the laser with much more intensity than these particles, preventing the CCD camera to capture the seeding particles. As usually recommended for the application of the PIV technique in gas-liquid flows, the LIF technique was employed, in which fluorescent seeding particles were used along with an optical filter in front of the CCD camera lens. Particles of Rhodamine B with $20 \mu\text{m}$ mean diameter were used, capable to receive light in a wavelength of 532 nm and emit (fluorescence) at 590 nm (peak). A high band pass filter for the wavelengths above 545 nm is used at the camera lens, filtering all the light at the laser wavelength (the same scattered by the interfaces) and capturing the light fluoresced by the seeding particles.

Due to the characteristics of the PIV method (Raffel *et al.*, 2007), specially in the cross-correlations algorithms used to generate the vectors, even when using the LIF technique, some interrogation windows occupied by bubbles produce acceptable vectors as can be seen in Fig. 2. This sort of error can introduce some sort of bias in the velocity fields, since the seed particles are only present in the liquid phase and appear to be in the gas phase due to reflections and light scattering. The inclusion of these unrealistic velocity vectors in the time averaging procedure overestimates the liquid velocity average field due to slip velocity between the dispersed bubbly gas and the liquid.

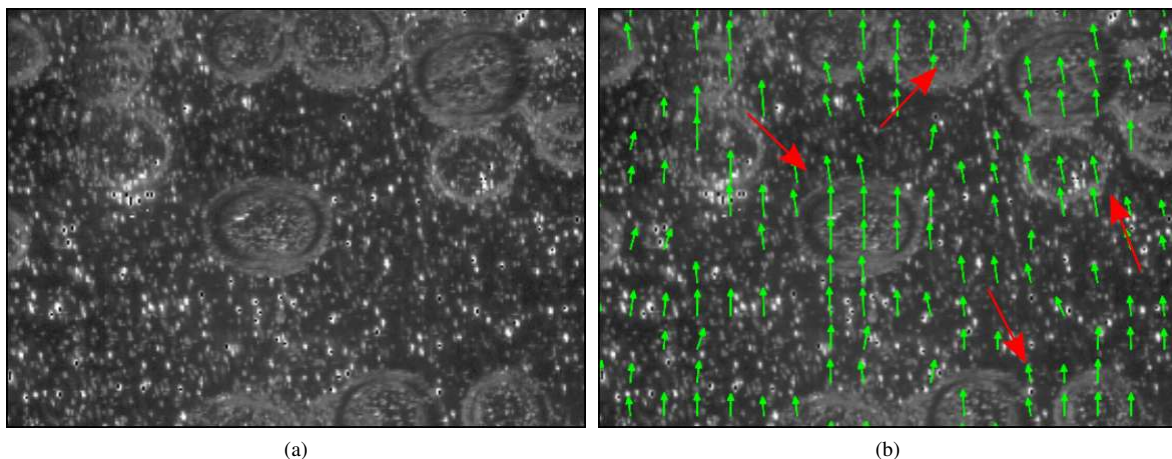


Figure 2: Problems caused by the presence of the bubbles within the PIV method. a) Raw image from the high-speed camera; b) Obtained velocity field from the non-treated image.

In order to remove these unrealistic velocity vectors, the next session is dedicated to describe the proposed method which can be used in bubbly flows with low to moderate void fractions without an excessive overestimation in the time averaged fields. It is also important to state that in the cases where dispersed bubbles are present, it is assumed that the seeding particles travel only in the liquid phase, thus any measured velocity vector corresponds to the liquid phase velocity.

4. IMAGE PROCESSING

The main goal for the proposed image processing technique is to identify the gas phase contributions from the original PIV images and therefore remove, due to the reasons mentioned in the previous paragraphs, the unrealistic velocity vectors which arises from off-plane illuminated particles or ghost particles. From the works found in the literature, it has been observed that most part of the described image processing methods (Lindken and Merzkirch, 2002; Bröder and Sommerfeld, 2002; Zhou *et al.*, 2013; Kim *et al.*, 2016) rely on image filtering and transformations techniques. These operations are performed in order to “mask out” the gas phase, creating new processed frames, that are then introduced in a cross-correlation PIV algorithm, resulting in the desired liquid velocity field.

The major contribution of the present work is the development of a phase discrimination method which does not rely on a masking procedure, but analyzes each velocity vector from the PIV cross-correlation algorithm and verifies the presence of the gas phase, as demonstrated in Fig. 3. The existence of a gas or liquid phase in each window is done by a series of processing steps in its pixel intensity values and will be described in the following paragraphs.

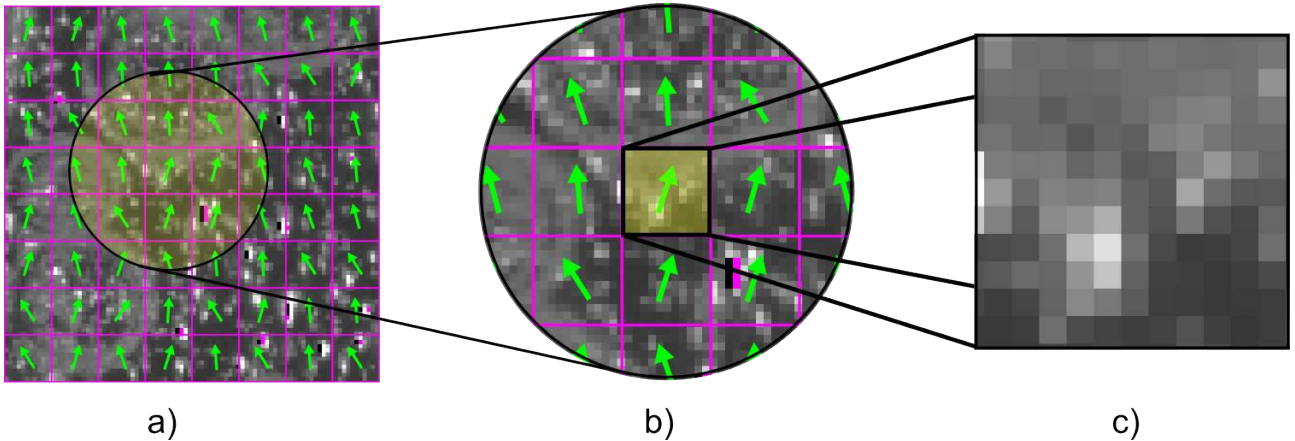


Figure 3: Phase discrimination procedure: a) A PIV frame, its original velocity vectors and the grid formed by the various interrogation windows; b) A close-up in the region surrounding a velocity vector; c) The interrogation window of the velocity show in b), where the phase discrimination sequence takes place.

From the PIV recordings, a first initial velocity field is obtained by the TSI Insight 4G software. These velocity fields and the PIV frames from each instantaneous acquisition are then used as input in an in-house developed image processing algorithm. This computer code then divides each 2048 x 2048 frame in a collection of 32 x 32 frames, the size of each interrogation window that will be used by the PIV algorithm classifying each window by its SNR value (valid vector if $SNR > 2.0$ and invalid vector if the criteria is not fulfilled) and then proceeding to the image processing steps.

In the first step, a Gaussian filter (3 x 3 size) is applied to remove part of the noise caused by the light reflections due to the presence of the dispersed bubbles, and also to “join” some seed particles that cluster due to gas phase, as shown in Fig. 4 by the operation A.

From the pixel intensity from the first step, the Otsu’s method (Otsu, 1975) is used to create a binary image, since the method determines an optimal pixel intensity value to define the threshold that classifies the image in two groups, in this case, black (pixel intensity value of 0) and white (pixel intensity value of 255). In Fig. 4 the procedure is shown in operation B.

In the last step (operation C in Fig. 4), which produces the final processed interrogation window images used for the phase discrimination, an erosion filter (2 pass) was applied to eliminate part of the noise produced by the interaction of the fluorescent seed particles and the gas phase.

By using this erosion filter, it is not possible to fully discriminate a dispersed bubble from the background and the seed particles. However, the image produced by this final step can be used as a parameter to define if an interrogation window contains information of the dispersed gas phase. The parameter P_1 , is calculated by Eq.

$$P_1 = \frac{\sum_{i=1..I} \sum_{j=1..J} IM_{erosion}[i, j]}{255 \cdot I \cdot J} \quad (1)$$

where, I and J represents the i and j dimension of the interrogation window ($I = J = 32$) and $IM_{erosion}$ is the image

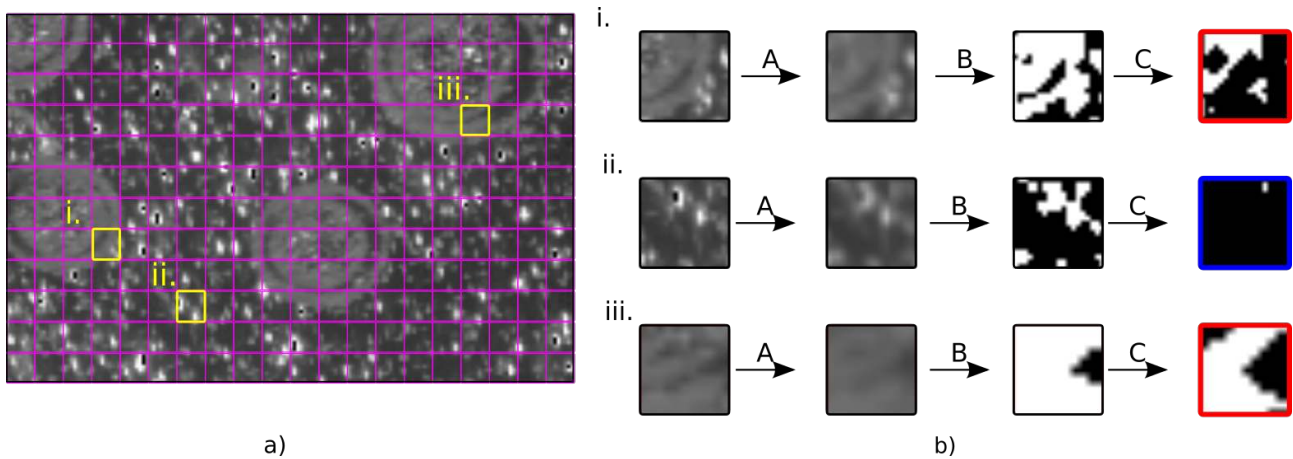


Figure 4: a) Original image from the PIV recording and the grid formed by the interrogation windows, highlighting sub-windows i.), ii) and iii). b) Image processing steps being performed in the interrogation windows highlighted in a), where operation A is the application of a Gaussian filter, operation B represents the Otsu's method and operation C is an erosion filter. As a result from the proposed method, interrogation windows i) and iii) are identified as being located in a gas-phase region.

obtained from the operation C (see Fig. 4). An interrogation window is identified as being located in a gas phase region when the parameter P_1 is above some certain threshold. The threshold value differs from case to case and depends on the quantity of dispersed bubbles in the flow and also the laser sheet's illumination power. Figure 5 illustrates the output of the in-house developed algorithm for three flow configurations considering three different values and gas flow rate (Q_G) with the same liquid flow rate (Q_L). In this picture, the gas-phase interrogation windows are shown in red, while the "uncontaminated" vector velocities are pictured by blue interrogation windows.

For certain cases, the proposed method described in the paragraphs above indicates false gas-phase interrogation windows. This can be observed in Figure 5a), where interrogations windows with the presence of only seed particles are being detected as a gas-phase windows. Nonetheless, this does not affect the effectiveness of the method, since all the gas-phase interrogation windows are treated as invalid vectors and are not take account in the averaging process. It is evident that the threshold requirement can be more strict, resulting in more invalid vectors being detected without the presence of a gas phase. In this case, more PIV measurements will be required to get consistent ensemble averages. In the results presented in the next section, 600 to 1000 PIV measurements were considered in the averaged fields.

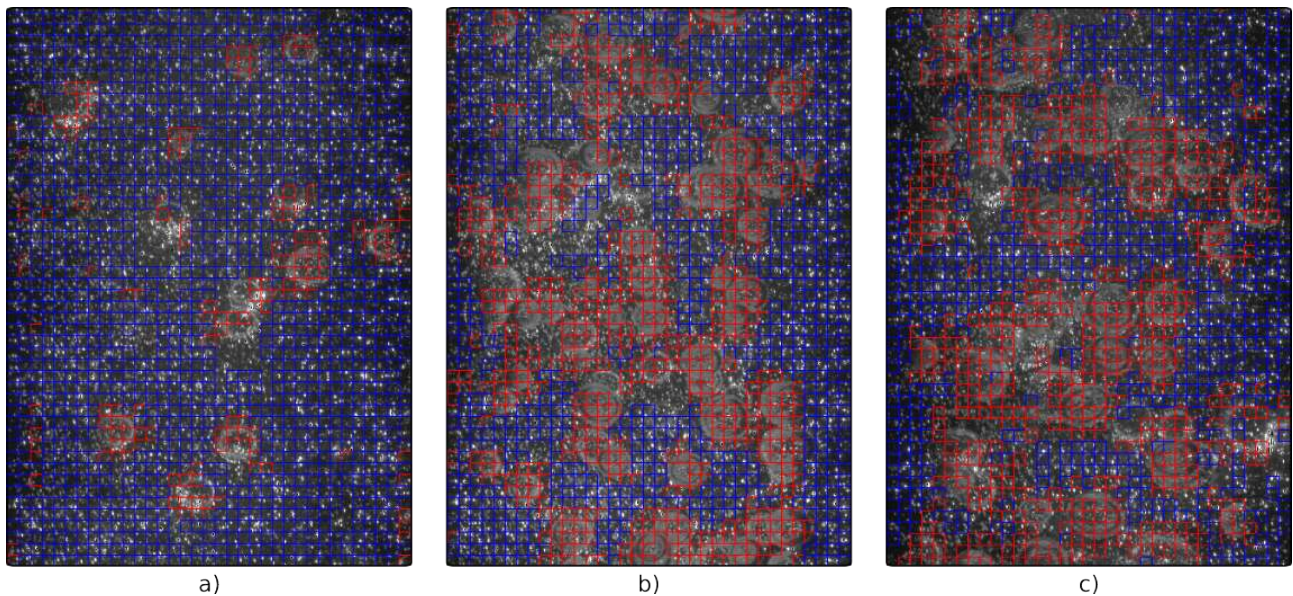


Figure 5: Original image from the PIV recording, in which the blue interrogation windows indicates presence of the liquid phase and the red ones the gas phase for three flow configurations: a) $Q_L = 390.0l/h$ and $Q_G = 8.80l/h$; b) $Q_L = 390.0l/h$ and $Q_G = 30.47l/h$ and c) $Q_L = 390.0l/h$ and $Q_G = 50.43l/h$

Figure 6 illustrates the instantaneous liquid velocity vectors obtained by the PIV processing before and after the application of the proposed method.

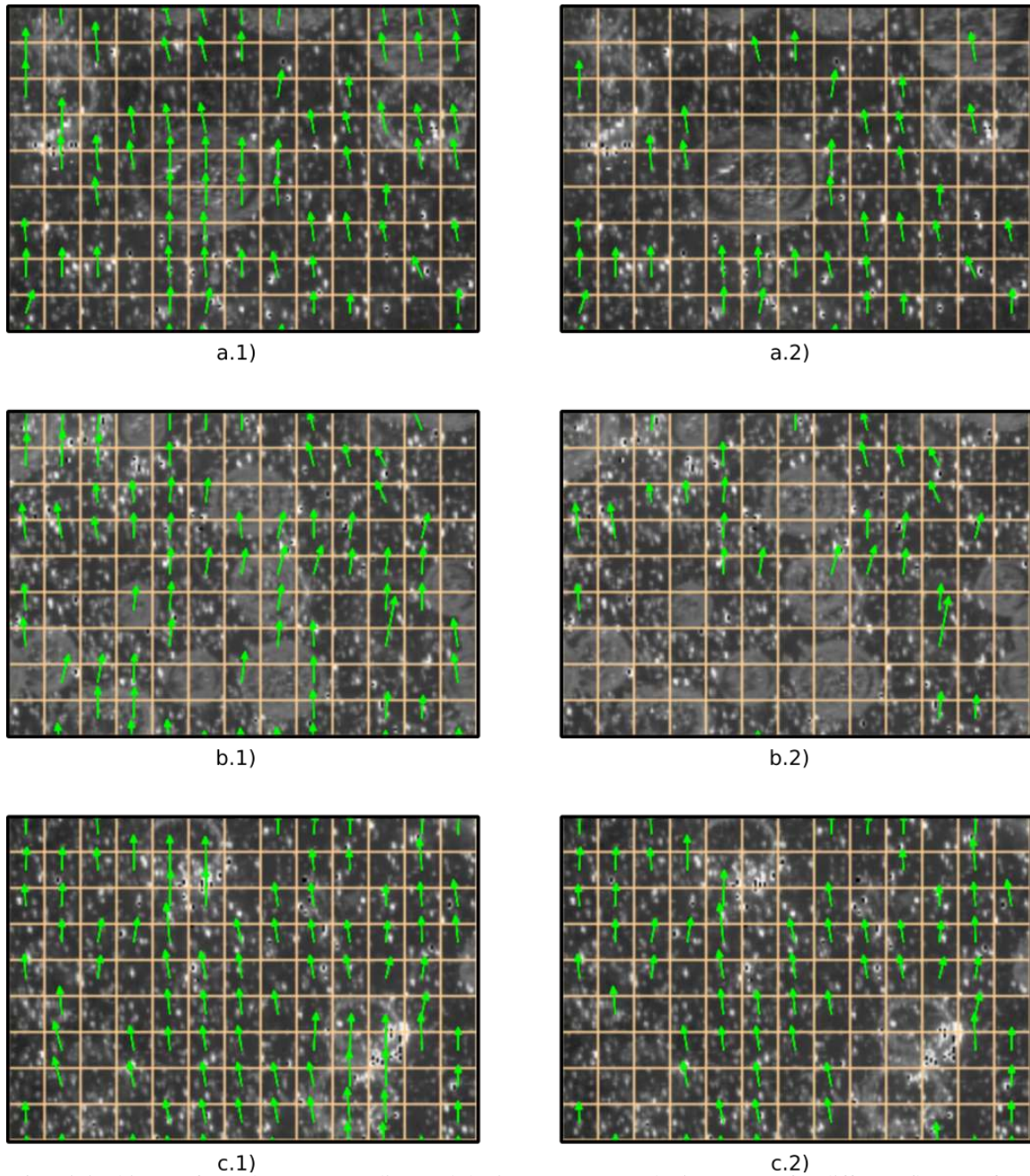


Figure 6: Original image from the PIV recording and the instantaneous velocity vectors for different flow configurations ($Q_L = 390.0\text{ l/h}$): a.1) $Q_G = 50.43\text{ l/h}$ and a.2) $Q_G = 50.43\text{ l/h}$; b.1) $Q_G = 30.47\text{ l/h}$ and b.2) $Q_G = 30.47\text{ l/h}$; c.1) $Q_G = 8.80\text{ l/h}$ and c.2) $Q_G = 8.80\text{ l/h}$

5. RESULTS

5.1 Validation of the PIV Results

The experimental set-up and instrumentation previously described were validated through various procedures. First, an experiment for single-phase flow conditions was developed and compared with solutions available in literature. In all cases, the averaged fields were calculated as the ensemble average as,

$$\langle v(r, z) \rangle = \frac{1}{N} \sum_{k=1}^N v_k(r, z) \quad (2)$$

In order to validate the PIV technique, mainly in terms of spatial calibration, results for single phase flow with $Q_L = 390.0\text{ l/h}$ are compared with results presented in literature, obtained with LDV and DNS Eggels *et al.* (1994). Figure 7

present a comparison of velocity profiles, made non-dimensional by the shear velocity v_τ , defined as,

$$\langle v(r, z) \rangle / v_\tau = \bar{v} \sqrt{\frac{0.0791 Re_L^{-1/4}}{2}} \quad (3)$$

where $Re_L = \bar{v}2R/\nu$ is the liquid Reynolds number and \bar{v} is the average liquid velocity, that can be calculate from the water flow meter as $\bar{v} = Q_L/\pi R^2$.

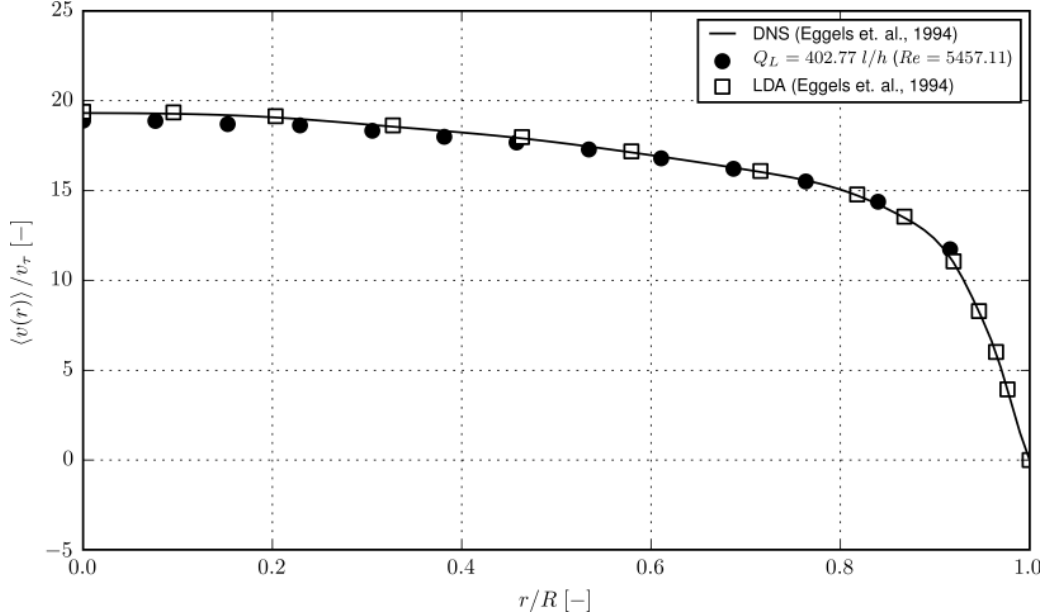


Figure 7: Comparison of velocity profiles for turbulent single phase flow.

In addition, the liquid flow rate calculated by integrating the measured velocity along the radial direction is compared with the measured flow rate, the integration of the $\langle v(r) \rangle$ resulted in a value of $Q_L^{PIV} = 402.77$ l/h, with an error of 3.27%, inside the flow meter accuracy range ($\pm 5.0\%$).

These results bring confidence on PIV measurements, mainly, in terms of spatial calibration.

5.2 Test Matrix

In this work, one single-phase flow condition and three two-phase flow conditions have been tested. The test matrix is shown in Table 1, where the liquid ($j_L = Q_L/\pi R^2$) and gas ($j_G = Q_G/\pi R^2$) superficial velocities were calculated based in the gas and liquid flow meters. The ratio between the liquid and gas flow is given by ($\beta = Q_G/(Q_G + Q_L)$).

Table 1: Test Matrix.

Experiment No.	Q_L [l/h]	Q_G [l/h]	j_L [m/s]	j_G [m/s]	β [-]
1	390.0	0.0	189.21×10^{-3}	0.0	0.0
2		8.38		0.41×10^{-2}	0.021
3		30.47		1.48×10^{-2}	0.072
4		50.43		2.47×10^{-2}	0.115

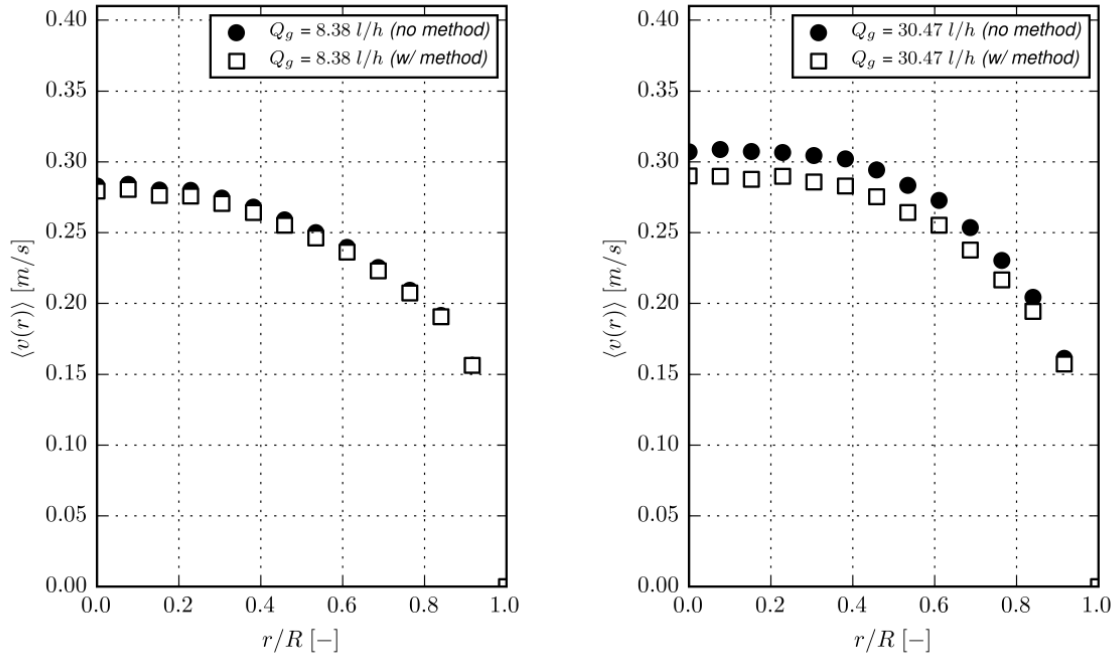
5.3 Results

The experiments given in Table 1 were performed with the PIV setup and cross-correlations configurations as those indicated in Section 2, and results presented here correspond to those in a position $z/D = 70$ away from the liquid inlet (see Fig. 1). To obtain the average liquid velocity profiles, the various frames were calculated as the ensemble average as,

$$\langle v(r) \rangle = \frac{1}{N} \sum_{k=1}^N v_k(r, z/D = 70) \quad (4)$$

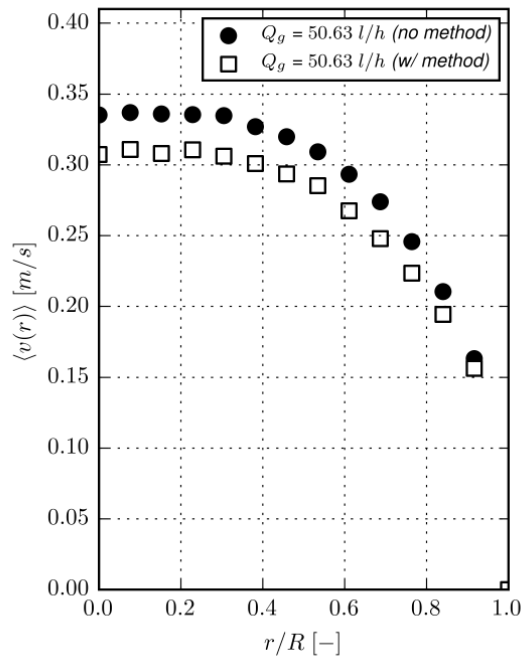
Figure 8 shows the average liquid velocity profiles obtained from the TSI Insight 4G software without the application of the processing method (no method) and after being processed by the in-house developed algorithm (w/ method), which uses the method proposed in this work.

As expected, from the results of Fig. 8, the difference due to the removal of the velocity vectors which have its interrogation windows occupied by the gas increases with gas superficial velocity, and the impact of the application of the method in the resulting averaged fields is higher.



(a) Experiment No. 2

(b) Experiment No. 3



(c) Experiment No. 4

Figure 8: Average radial liquid velocity profiles from the configurations show in Tab. 1. The profiles are presented with and without the use of the method proposed in this work.

As expected, the processed results in lower upward vertical velocities, since a major part of the bias from the dispersed bubbles are removed. In addition, from Figure 9 the non-removal of these "spurious" liquid velocity can lead to substantial errors, up to 9% in cases with a considerable quantity of gas ($\beta > 0.1$). In order to calculate the difference caused by the

use of the proposed method, the values are plotted with $\langle v_{diff}(r) \rangle$,

$$\langle v_{diff}(r) \rangle = 100\% \frac{\langle v(r) \rangle |_{no\ meth.} - \langle v(r) \rangle |_{w/ meth.}}{\langle v(r) \rangle |_{no\ meth.}} \quad (5)$$

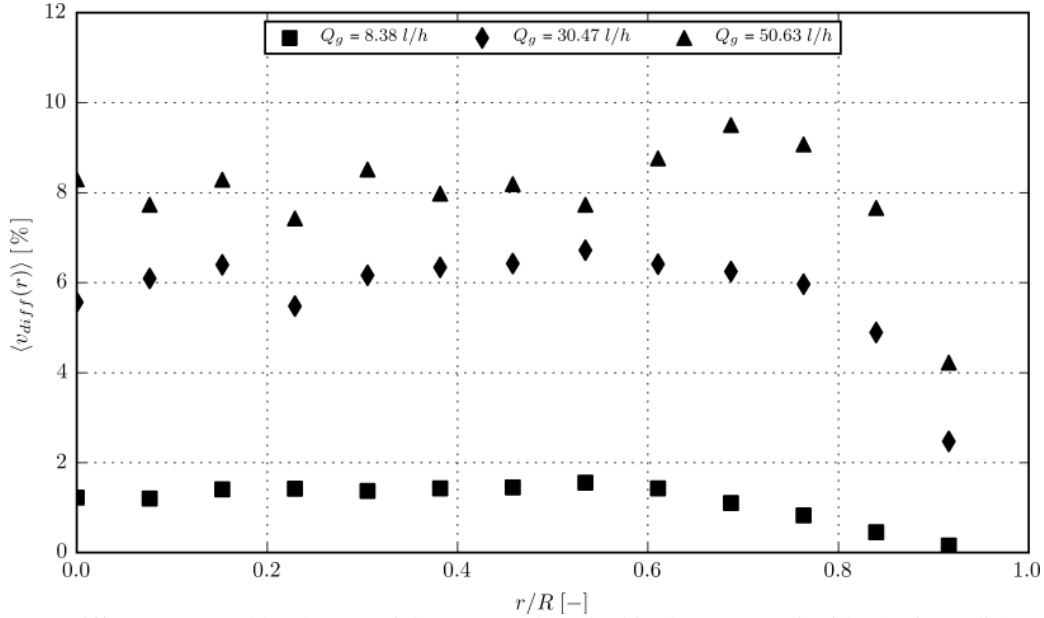


Figure 9: Difference caused by the use of the proposed method in the average liquid velocity radial profile.

The results presented above proves that the method is well suited for dealing with two-phase flows with a considerable quantity of gas and is capable of extract the average liquid velocity vector from PIV frames. Since it is possible to extract information about the liquid velocity, the void fraction α can be calculated through the relation,

$$\alpha_G = 1.0 - \frac{J_L}{\langle \overline{v(r)} \rangle} \quad (6)$$

where $\langle \overline{v(r)} \rangle$ is calculated as,

$$\langle \overline{v(r)} \rangle = \frac{1}{\pi R^2} \int_0^{2\pi} \int_0^R \langle v(r) \rangle r d\theta dr \quad (7)$$

Figure 10 shows how the void fraction α changes with the gas superficial velocity, J_G . It is interesting to note how the void fraction is overestimated when the proposed method is not applied in the instantaneous liquid velocity field, with differences of more the 50% in situations with moderate an high gas quantity.

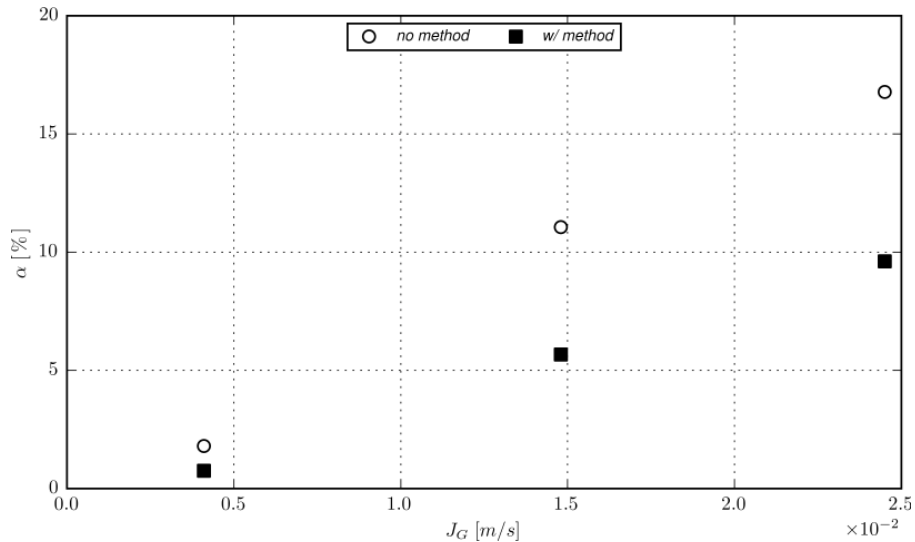


Figure 10: Void fraction α for different experiment runs from Tab. 1.

6. CONCLUSION

The PIV/LIF technique is a commonly used technique for measurement in air-water flow configurations, since it can be used to discriminate the dispersed gas phase and the tracer particles presents in the liquid. However, for moderate to high gas fractions, the technique cannot be used without a phase discrimination method, as the light scattered by the gas bubbles can generate spurious vector velocities in the PIV cross-correlation step.

In this work, a new method for phase discrimination was proposed to overcome the issues that occurs when the PIV/LIF technique is used as a measurement technique in vertical air-water two-phase flows inside ducts. The method is based in a phase discrimination procedure which classifies the PIV obtained vector velocities by its interrogation window pixel information. A single-phase flow experiment was conducted in order to verify the experiment setup and the spatial calibration used in this work.

In order to assess the effectiveness of the new method, three air-water experiments were studied, ranging from low to moderate gas quantities. From the two-phase experiments it is shown that the proposed method can filter out the spurious vector velocities originated from the gas-phase in the PIV recordings. The comparison of the ensemble averaged vector fields demonstrates that without the correct phase discrimination process, the liquid velocities and the gas void fraction can be overestimated.

7. ACKNOWLEDGEMENTS

This work was realized with the financial support of the Brazilian National Petroleum Agency - ANP, through Human Resources Program of ANP for Petroleum and Natural Gas

8. REFERENCES

- Bröder, D. and Sommerfeld, M., 2002. "An advanced LIF-PLV system for analysing the hydrodynamics in a laboratory bubble column at higher void fractions". *Experiments in Fluids*, Vol. 33, pp. 826–837. ISSN 0723-4864. doi: 10.1007/s00348-002-0502-z.
- Bröder, D. and Sommerfeld, M., 2007. "Planar shadow image velocimetry for the analysis of the hydrodynamics in bubbly flows". *Measurement Science and Technology*, Vol. 18, No. 8, pp. 2513–2528. ISSN 0957-0233. doi:10.1088/0957-0233/18/8/028.
- Eggels, J.G., Unger, F., Wiess, M.H., Westerweel, J., Adrian, R.J., Friedrich, R. and Nieuwstadt, F.T.M., 1994. "Fully Developed Turbulent Pipe Flow: A Comparison Between Direct Numerical Simulation and Experiment". *J. Fluid Mech.*, Vol. 268, pp. 175–209.
- Fujiwara, A., Minato, D. and Hishida, K., 2004. "Effect of bubble diameter on modification of turbulence in an upward pipe flow". *International Journal of Heat and Fluid Flow*, Vol. 25, No. 3, pp. 481–488. ISSN 0142727X.
- Hosokawa, S. and Tomiyama, A., 2013. "Bubble-induced pseudo turbulence in laminar pipe flows". *International Journal of Heat and Fluid Flow*, Vol. 40, pp. 97–105. ISSN 0142727X. doi:10.1016/j.ijheatfluidflow.2013.01.004.
- Kim, M., Lee, J.H. and Park, H., 2016. "Study of bubble-induced turbulence in upward laminar bubbly pipe flows measured with a two-phase particle image velocimetry". *Experiments in Fluids*, Vol. 57, No. 4, p. 55. ISSN 0723-4864. doi:10.1007/s00348-016-2144-6.
- Lindken, R. and Merzkirch, W., 2002. "A novel PIV technique for measurements in multiphase flows and its application to two-phase bubbly flows". *Experiments in Fluids*, Vol. 33, No. 6, pp. 814–825. ISSN 0723-4864. doi:10.1007/s00348-002-0500-1.
- Otsu, N., 1975. "A threshold selection method from gray-level histograms". *Automatica*, Vol. 11, No. 285-296, pp. 23–27.
- Raffel, M., Willert, C.E., Wereley, S.T. and Kompenhans, J., 2007. *Particle Image Velocimetry*, Vol. 79. ISBN 9783540723073.
- Sun, X., Paranjape, S., Ishii, M. and Uhle, J., 2004a. "LDA measurement in air-water downward flow". *Experimental Thermal and Fluid Science*, Vol. 28, No. 4, pp. 317–328. ISSN 08941777. doi:10.1016/S0894-1777(03)00105-5.
- Sun, X., Paranjape, S., Kim, S., Ozar, B. and Ishii, M., 2004b. "Liquid velocity in upward and downward air-water flows". *Annals of Nuclear Energy*, Vol. 31, No. 4, pp. 357–373. ISSN 03064549. doi:10.1016/j.anucene.2003.08.002.
- Zhou, X., Dou, B. and Sun, X., 2013. "Measurements of liquid-phase turbulence in gas-liquid two-phase flows using particle image velocimetry". *Measurement Science and Technology*, Vol. 24, No. 12, p. 125303. ISSN 0957-0233.

9. RESPONSIBILITY NOTICE

The authors are the only responsible for the printed material included in this paper.